All-Graphene Core-Sheath Microfibers for All-Solid-State, Stretchable Fibriform Supercapacitors and Wearable Electronic Textiles

*Yuning Meng, Yang Zhao, Chuangang Hu, Huhu Cheng, Yue Hu, Zhipan Zhang, Gaoquan Shi, and Liangti Qu**

Flexible graphene fiber (GF) stands for a new type of fiber of practical importance, which integrates such unique properties as high strength, electrical and thermal conductivities of individual graphene sheets into the useful, macroscopic ensembles. GFs possess the common characteristics of fibers like the mechanical flexibility for textiles, while maintaining the uniqueness such as low cost, light weight, and ease of functionalization in comparison with conventional carbon fibers.[1–3] Due to the extraordinary challenge to assemble two-dimensional (2D) microcosmic graphene sheets with irregular size and shape into macroscopic fibrillar configuration, however, the success in fabrication of neat graphene fibers only comes true recently.[1–4] In this regard, we have devised a facile one-step dimensionally-confined strategy to fabricate the neat GFs by directly hydrothermally assembling graphene within glass pipeline.[2,5] The as-produced GFs have a density of 0.23 g/cm^3, 7 times and 85 times lower than that of conventional carbon fibers (>1.7 g/cm^3) and Au wire (ca. 20 g/cm^3), while remaining strong, flexible, conductive, weavable and shapeable, and their engineered structures with multifunctionalities can be done readily in an in situ or post-synthesis fashion.[2] These remarkable features of GFs endow them with prominent advantages over common carbon fiber and metal wires[6] for development of unconventional, lightweight, flexible devices, especially in fiber shape for wearable electronics.

The flourishing progress of electronics in the unconventional forms has opened a new prospect of future electronics such as smart skins, human friendly devices, and flexible/stretchable circuitries and energy devices.[7–16] This new class of electronics can conformably deform into complex, non-planar shapes under bending, stretching, compressing, twisting process while maintaining good performance, reliability and integration. Flexible energy-storage devices have attracted tremendous attentions in recent years due to their promise in integration into stretchable and wearable electronics.[7,17–23] In particular, supercapacitors are of significant interest as energy storage devices associated with their high power density, long cycling life, and short charging time.[24,25] Conventional supercapacitors are heavy and bulky, targeting for the applications in electric or hybrid vehicles, and auxiliary power sources. However, the development of high-efficiency miniaturized supercapacitor devices compatible with the flexible and wearable electronics lags except from several recent paradigms.[26–30]

3D graphene structures possess notable features including highly-exposed surface areas, high electrical conductivity, and good chemical stability, and therefore they have been widely explored as electrode materials for supercapacitor applications.[31–35] Herein, we design and fabricate a unique all-graphene core–sheath fiber, in which a core of GF is covered with a sheath of 3D porous network-like graphene framework. This hierarchical hybrid structure is denoted as GF@3D-G. The high electronic conduction of the core graphene fiber and the highly exposed surface areas of 3D graphene network are well combined within the GF@3D-G, thus offering the great advantages as flexible electrodes for efficient fiber-based electrochemical supercapacitor. The fiber supercapacitors comprise two intertwined electrodes, both of which are solidified in the H_2SO_4-polyvinyl alcohol (PVA) gel electrolyte for formation of an all-solid-state fiber supercapacitor. The assembled fiber supercapacitor of GF@3D-G is highly flexible, which can be managed to spring supercapacitor with highly compressible and stretchable properties, and can also be conveniently woven into a textile for wearable electronics as demonstrated below.

The all-graphene GF@3D-G structure was prepared by directly electrochemically electrolyzing 3 mg mL^{-1} graphene oxide (GO) aqueous suspension containing 0.1 M lithium perchlorate ($LiClO_4$) on GFs at an applied potential of −1.2 V for 5 min (see Experimental for details).[36,37] The flexible GFs were generated as reported in our previous paper,[2] which have a diameter of ca. 30 μm with a typical electric conductivity of ca. 10 S/cm, similar to those of spun carbon nanotube fibers.[38,39] Just like the initial GFs, the as-produced GF@3D-G is also flexible enough to intertwine ad arbitrium (**Figure 1**a). The GF@3D-G has a relatively larger tensile strength than that of the initial GF (Figure S1), indicating the growth of 3D-G along GF does not impair the intrinsic mechanical property of GF. During the electrolyzing process, GO sheets were reduced into conductive graphene and self-assembled into 3D interpenetrating

Y. Meng, Y. Zhao, C. Hu, H. Cheng, Yue Hu,
Dr. Z. Zhang, Prof. L. Qu
Key Laboratory of Cluster Science
Ministry of Education, School of Chemistry
Beijing Institute of Technology, Beijing 100081, China
E-mail: lqu@bit.edu.cn
Prof. G. Shi
Department of Chemistry
Tsinghua University
Beijing 100084, China

DOI: 10.1002/adma.201300132

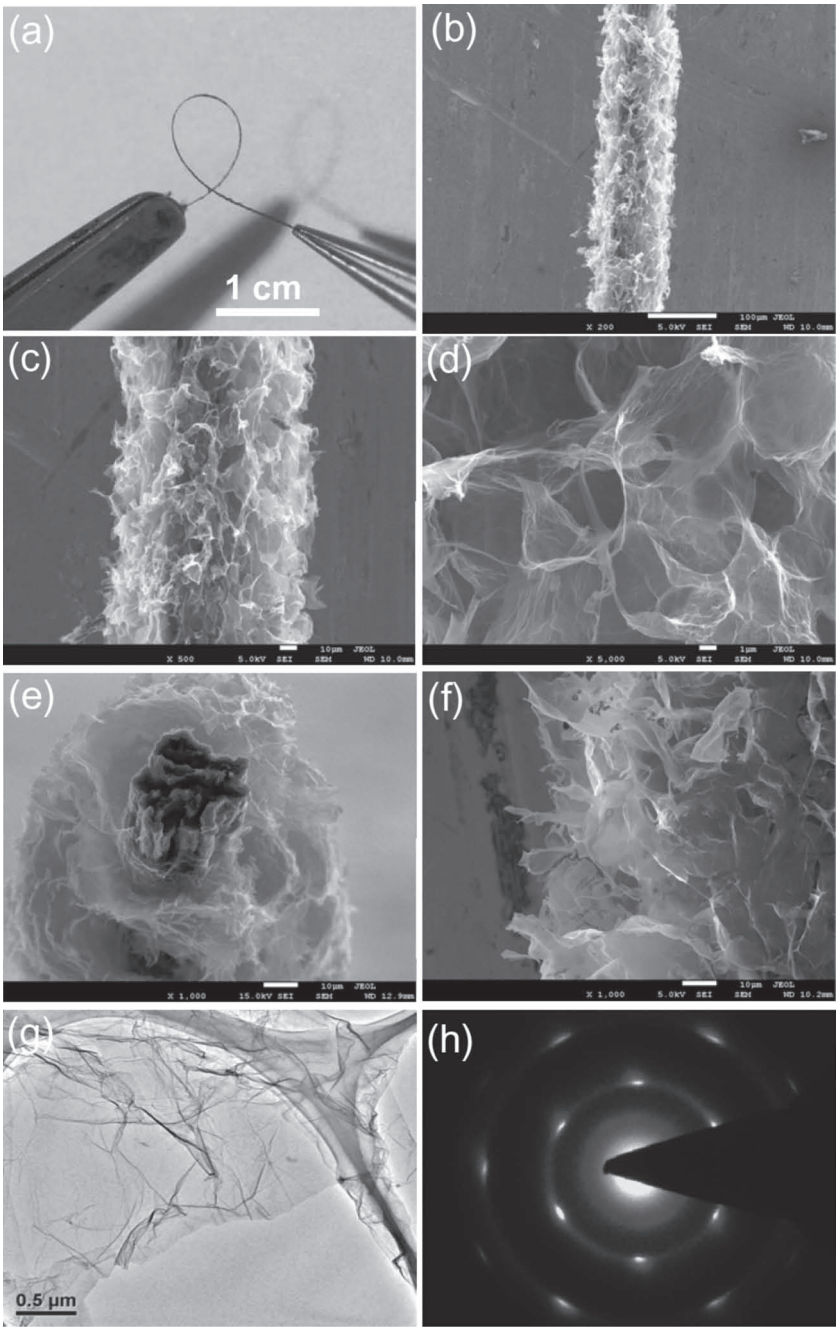

Figure 1. (a) A photo of a distorted GF@3D-G. The observed particle-like bulging along the intersectant fiber results from the fiber-fiber attrition contact during manual distortion. (b, c) SEM images of a GF@3D-G. (d) An enlarged view of (c). (e) Cross-section view of a GF@3D-G showing the core GF surrounding with standing graphene sheets. (f) The edge view of a GF@3D-G. (g and h) TEM image of deposited graphene sheets on GF and the corresponding selected area electron diffraction of graphene sheet. Scale bars: b, 100 μm; c,e,f, 10 μm; d, 1 μm; g, 0.5 μm.

networks on GF electrode under the driving force of electric field (Figure 1b–f).[36] X-ray photoelectron spectroscopy (XPS) analysis indicates that most of the oxygenated functional groups of GO have been removed by electrochemical reduction (Figure S2). As a result, GF@3D-G has a typical conductivity of ca. 10–20 S/cm, slightly higher than that of GF. The deposited graphene layers are uniformly distributed along the whole fiber with pore-rich structure (Figure 1b,c). The pore sizes of the network are in the range of several micrometers to larger than ten micrometers (Figure 1d). The cross-section view clearly shows the deposited graphene sheets encompass the core GF with the graphene planes nearly directional to the GF surface (Figure 1e,f), which largely facilitates the sufficient exposure of graphene sheets to the electrolyte for the access of ions to form electrochemical double-layers. The deposited graphene sheets tightly surround the core GF (Figure S3), which provides the mechanical stability of GF@3D-G under deformation (Figure S4). TEM image displays the deposited graphene sheets on GF are almost transparent under electron irradiation, and electron diffraction pattern presents the symmetric diffraction spots, suggesting the high quality of graphene crystalline structure.

To test the electrochemical performance of GF@3D-G, we first investigate the cyclic voltammetry (CV) response of a single GF@3D-G fiber in comparison with the pure GF in a three-electrode electrochemical cell. As shown in **Figure 2**a, the GF@3D-G electrode exhibits the CV curves of nearly rectangular shape, showing ideal capacitive behavior under the measured scan rate from 30 mV/s to 500 mV/s, which probably results from the highly conductive and surface-exposed graphene network directly coated on the GF, accessible for fast ion transportation. In contrast, the pure GF presents the significantly compressed current-voltage curves in shuttle-like shape within the different scan rates (Figure 2b). These results show the ineffective ion transport occurred on the compact GF in contrary to the porous GF@3D-G and GF mainly worked as the current collector.

Based on the great capacitive behavior and the high flexibility of GF@3D-G, we build the flexible all-solid-state fiber supercapacitor by intertwining two GF@3D-G electrodes with H_2SO_4-PVA gel polyelectrolyte (**Figure 3**a). The specifically selected solid-state electrolyte for the fiber supercapacitor will overcome the major drawbacks of conventional liquid electrolytes, such as leakage of electrolyte, difficulty in device integration and environmental stability, which are crucial for the development of useful wearable fiber devices. Apart from acting as the electrolyte, the coating layer of H_2SO_4-PVA gel along the whole GF@3D-G could also function as an effective separator to prevent the undesirable short circuit of two electrodes.

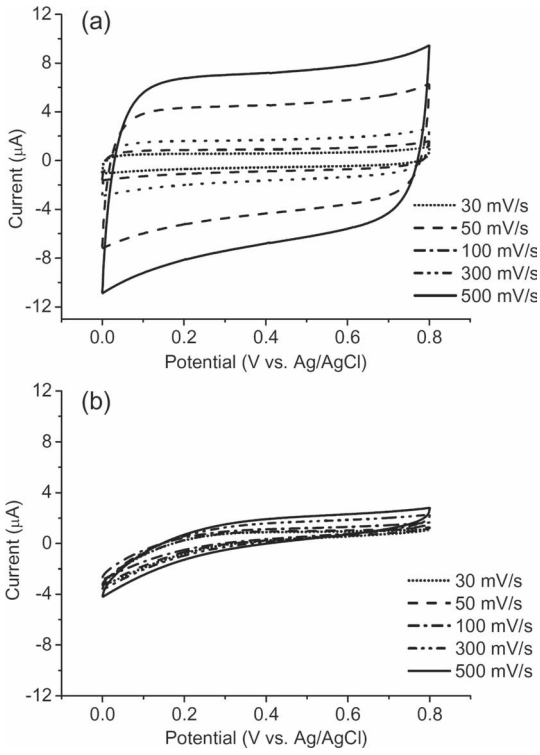

Figure 2. CV curves of a 1-cm-long GF@3D-G (a) and GF (b) in 1 M $LiClO_4$ aqueous solution under different scan rates.

The resulting supercapacitor maintains good fiber shape (Figure 3b) and has an excellent flexibility similar to the single GF@3D-G (Figure 3c). The intertwining structure of two GF@3D-G electrodes covered with H_2SO_4-PVA gel electrolyte is shown in Figure 3d. The GF@3D-G surfaces become smooth due to the uniform coating of electrolyte gel (Figure 3d,e). The enlarged view of the deliberately broken fiber shows that the electrolyte has been fully infiltrated into the 3D-G layer and enwrapped the whole GF@3D-G, while maintaining the network structure of 3D-G undamaged (Figure S5).

The electrochemical properties of the fiber capacitor were characterized by CV and galvanostatic charge–discharge measurements. The CV curves keep a quasi-rectangular shape at scan rates of 30–500 mV s^{-1} (Figure S7), confirming the formation of an efficient electric double layers (EDLs) and good charge propagations between the electrodes. The contact interface area of two fiber electrodes coated with gel electrolyte can ensure the effective ion diffusion process for capacitor application (Figure S8). Almost overlapped CV curves are observed for the GF@3D-G fiber supercapacitor deformed from the straight to the bending status, and back to the straight again (Figure 3f and Figure S6). This is also the case for the charge–discharge curves with a typical triangular shape (Figure 3g), demonstrating the high flexibility and electrochemical stability of the fiber supercapacitor.

The flexible feature of the assembled fiber supercapacitor makes it robust to tolerate the long-term and repeated straight-to-bending process. As shown in Figure 3h,i, the fiber supercapacitor keeps a stable capacitance of ca. 30–40 μF whether in the bending or straight status during 500 cycles, indicating the excellent stability of the GF@3D-G supercapacitor under deformation. On the basis of the surface areas of the gel electrolyte coated GF@3D-G, the measured area-specific capacitance is ca. 1.2–1.7 mF/cm^2 (Figure S9), which exceeds that of fibre-shaped solid supercapacitor based on ZnO nanowires/graphene films (0.4 mF/cm^2),[27,40] graphene/Au wire (ca. 0.7 mF/cm^2),[6] and comparable to the values reported for electrochemical micro-supercapacitors (0.4–2 mF/cm^2).[41–43] The GF@3D-G supercapacitor has a mass-specific capacitance of ca. 25–40 F/g (Figure S10), which is lower than that of 3D graphene electrodes (>100 F/g),[31] but is still close to the electric double layer capacitance of activated carbon textiles (25–70 F/g),[44] similar to that of fiber supercapacitors utilizing pen ink as active materials (20–36 F/g),[30] and comparable to that of multi-layer graphenes/Xerox paper-based supercapacitor (23 F/g).[45] The energy and power densities of carbon-based and metal oxide–based supercapacitors reported by other groups are 10^{-6}–10^{-4} Wh/cm^2 and 10^{-3} to 10^{-1} W/cm^2, respectively.[27,46,47] The energy density and power density of GF@3D-G supercapacitor are 0.4–1.7 × 10^{-7} Wh/cm^2 and 6–100 × 10^{-6} W/cm^2 (Figure S11),

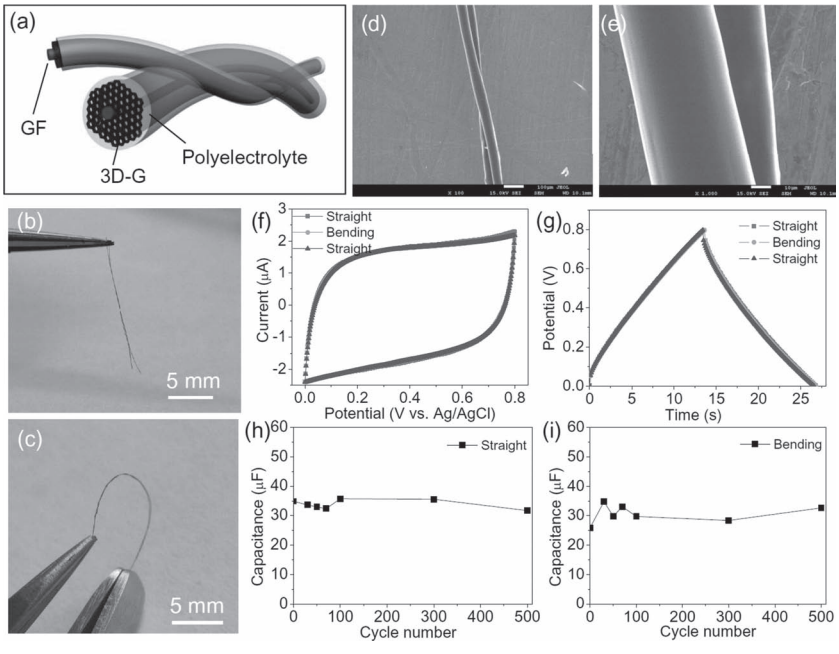

Figure 3. (a) Schematic illustration of a wire-shaped supercapacitor fabricated from two twined GF@3D-Gs with polyelectrolyte. (b,c) Photos of GF@3D-G fiber supercapacitor in free and bending state. (d,e) SEM images of the twined structure of GF@3D-Gs coated with polyelectrolyte under different magnification. (f,g) CV and charge-discharge curves of a 1.5-cm-long GF@3D-G fiber supercapacitor in straight and bending (bending radius of ~2 mm) states (Figure S6), respectively. The scan rate in (f) is 50 mV/s. The applied current in (g) is 2 μA. (h,i) The capacitance stability of GF@3D-G fiber supercapacitor in bending and straight state undergoing 500 straight-bending cycles, respectively.

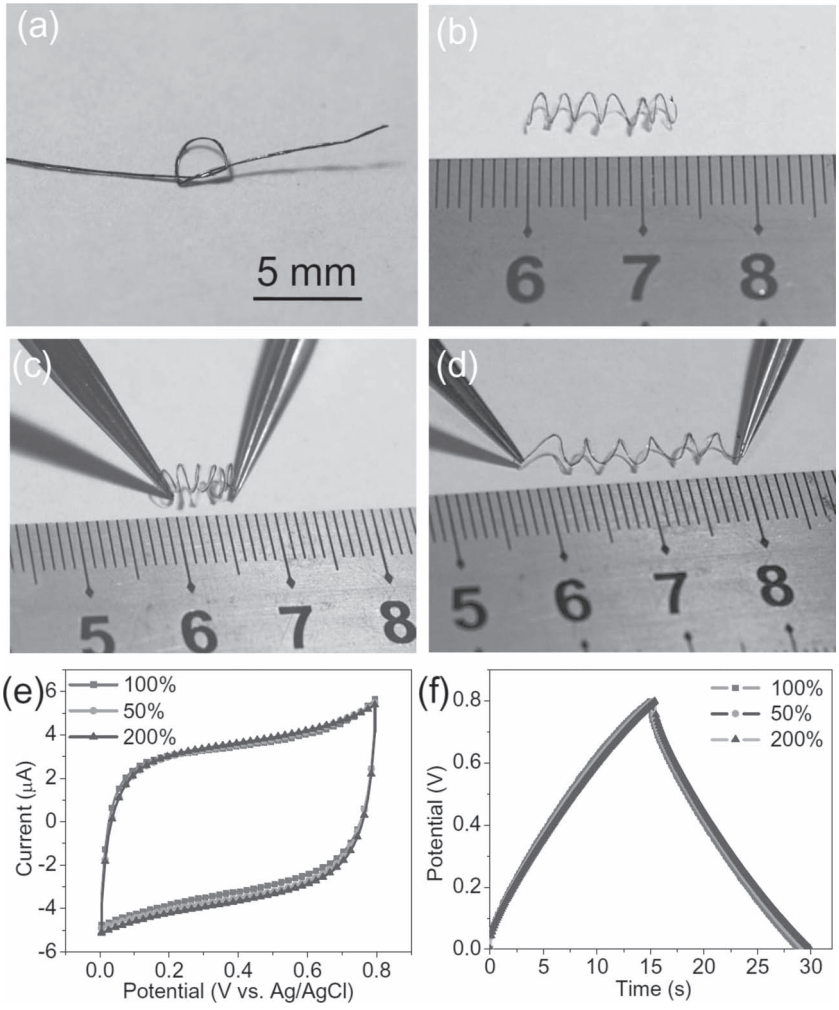

Figure 4. (a) A photo of the knotted fiber supercapacitor of GF@3D-Gs. (b–d) The spring-like supercapacitor with an effective GF@3D-G length of ca. 4.5 cm at free (100%), compressed (ca. 50%), stretched (ca. 200%) status, respectively. (e and f) The corresponding CV and charge-discharge curves of the spring-like supercapacitor at free (100%), compressed (ca. 50%) and stretched (ca. 200%) status, respectively. The scan rate in (e) is 50 mV/s. The applied current in (f) is 4 μA.

respectively, which are slightly lower than those reported carbon-based supercapacitors, but still comparable to that of ZnO nanowire-based fiber supercapacitor (Energy density: 2.7 $\times$ 10^{-8} Wh/cm^2, power denstiy: 1.4 $\times$ 10^{-5} W/cm^2).[27] Considering the special one-dimensional fiber configuration of the GF@3D-G supercapacitor, the calculated length-specific capacitance is ca. 20 μF/cm. It is also observed that the capacitance has an approximately linear increase with the length increase of GF@3D-G supercapacitor (Figure S12), indicating the uniformity and the scalable possibility of the fiber supercapacitor.

The flexible and mechanically stable fiber supercapacitor can be managed in a well-controlled way. As shown in **Figure 4**a, a knot of fiber supercapacitor has been conveniently made manually. Even in knotted state, the fiber supercapacitor has still a capacitance of ca. 19 μF/cm (Figure S13) consistent with the straight ones. A spring-like supercapacitor can also be fabricated by wrapping the "wet" fiber supercapacitor, that the H_2SO_4-PVA gel was freshly coated along the GF@3D-Gs, around a glass rod (Figure S14). After annealing at the room temperature for several hours, the spring-like supercapacitor is obtained (Figure 4b). This spring supercapacitor is compressible and stretchable (Figure 4c,d). At either cases, the spring supercapacitor presents a similar CV and charge-discharge features to that of the initial one (Figure 4e,f). As a result, all of them have a length-specific capacitance of ca. 18 μF/cm and an area-specific capacitance of ca. 1.2 mF/cm^2, which are close to that of fiber supercapacitor mentioned above.

To further demonstrate the application of the fiber supercapacitor in portable devices such as electronic textile or clothing integrated devices, we incorporated the fiber supercapacitor into a textile by a conventionally weaving technology. As shown in **Figure 5**a, two GF@3D-G fiber supercapacitors have been woven into a textile with embedded Cu wire as connecting electrodes. This fiber supercapacitor integrated textile maintains its inherent flexibility (Figure 5b) without loss of the capacitive performance (Figure 5c) in despite of the repeated bending process, indicating the reliability of GF@3D-G fiber supercapacitors for applications in integrated electronic textiles.

In summary, we have designed and fabricated a unique all-graphene core–sheath fiber composed of GF core with a sheath of 3D graphene network. This hierarchical all-graphene hybrid structure inherits the intrinsic high conductivity and mechanical flexibility of GF in combination with highly exposed surfaces of graphene sheets, thus offering the great advantages as flexible, lightweight electrodes for efficient fiber-based electrochemical supercapacitor. The all-solid-state fiber supercapacitor built on the basis of H_2SO_4-PVA gel electrolyte can be managed to spring-shaped supercapacitor with highly compressible and stretchable properties, and can also be woven into a textile for wearable electronics. This work represents a new hierarchical all-graphene GF@3D-G fiber electrode material for various electronic devices beyond those demonstrated in this study.

Experimental Section

GO was prepared from natural graphite powder *via* acid-oxidation as mentioned in our previous papers.[48–50] GF was fabricated by a facile one-step dimensionally-confined hydrothermal strategy from aqueous suspensions (Figure S15).[2] The preparation of GF@3D-G was carried out by electrolyzing 3 mg mL^{-1} GO aqueous suspension (pH = 3.62) containing 0.1 M $LiClO_4$, where GF with a diameter of ca. 30–35 μm and a certain length (typically, 2–10 cm) was directly utilized as working electrode, and Pt wire (1 mm in diameter) and Ag/AgCl (3 M KCl) were

ADVANCED MATERIALS
www.advmat.de

www.MaterialsViews.com

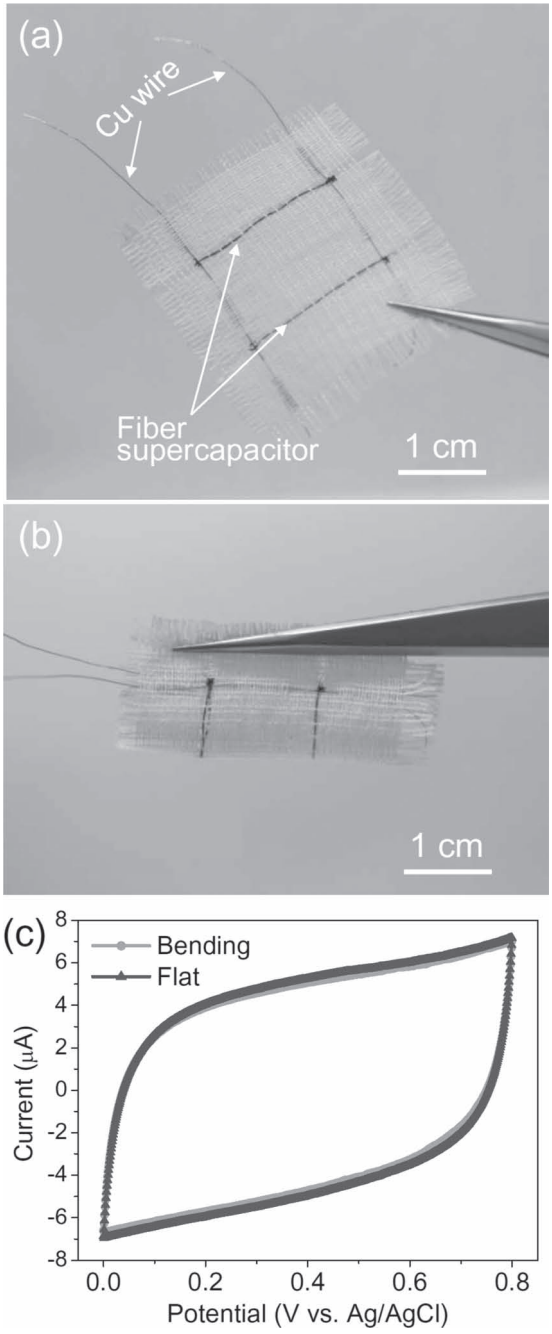

Figure 5. (a,b) Photos of the textile embedded with two GF@3D-G fiber supercapacitors (ca. 2 cm in length for each of them) in flat and bending state, respectively. (c) CV curves of two GF@3D-G fiber supercapacitors as the textile in flat (a) and bending (b) states with a scan rate of 50 mV/s.

used as counter and reference electrodes (Figure S16), respectively. A constant potential of –1.2 V was applied with a period of 5 min using a CHI660D electrochemical workstation (Figure S17). The as-prepared GF@3D-G was fully washed with distilled water and freeze-dried for further use.

The electrochemical behavior of single GF@3D-G in comparison with GF was tested in a three-electrode system in 1M $LiClO_4$ aqueous solution, where GF@3D-G in comparison with GF acted as working electrodes, Pt wire and Ag/AgCl (3 M KCl) were used as counter and reference electrodes, respectively.

The flexible all-solid-state fiber supercapacitor was fabricated by intertwining two GF@3D-G electrodes pre-coated with H_2SO_4-PVA gel polyelectrolyte. H_2SO_4-PVA gel electrolyte was simply made as follows: In a typical process, 6 g H_2SO_4 was mixed with 60 mL deionized water and then 6 g PVA powder was added. The whole mixture was heating up steadily to ~85 °C under vigorous stirring until the solution became clear. Then the solution was kept at 85 °C without stirring.

The capacitance C was calculated by using the equation: $C = I/(dV/dt)$, where I and dV/dt are the discharge current and the slope of the discharge curve. The area-specific capacitance C_A was derived from the equation: $C_A = C/A$, where A is the surface area of the fiber electrode and is equal to π multiplied by the diameter of the fiber electrode (D) and the device length (L).[30] The mass-specific capacitance C_m was calculated from the equation: $C_m = 2C/m$,[34,51,52] where m is the mass of one electrode. The length-specific capacitance C_L was derived from the equation: $C_L = C/L$, where L is the length of a fiber supercapacitor. The energy density (E) and power density (P) of the GF@3D-G supercapacitor can be obtained from $E = 0.5C_AV^2$ and $P = E/t_{discharge}$, where V represents the operating voltage and $t_{discharge}$ is the discharge time.

The morphologic characterization of GF@3D-G was carried out by JEM-2010 high resolution transmission electron microscopy (HR-TEM) at an acceleration voltage of 120 kV. Field-emission scanning electron microscope (FE-SEM) images the samples were taken on JSM-7001F SEM unit. Mechanical property test of μGT was conducted with an Instron material testing system (Instron 3342). The strain rate for a centimeter gauge length is 1 mm/min with a preload of 0.5 N.

Supporting Information

Supporting Information is available from the Wiley Online Library or from the author.

Acknowledgements

We thank the financial support from the 973 project (2011CB013000) of China and NSFC (21174019, 51161120361).

Received: January 10, 2013
Published online: March 6, 2013

[1] Z. Xu, C. Gao, *Nat. Commun.* **2011**, *2*, 571.
[2] Z. L. Dong, C. C. Jiang, H. H. Cheng, Y. Zhao, G. Q. Shi, L. Jiang, L. T. Qu, *Adv. Mater.* **2012**, *24*, 1856.
[3] H. P. Cong, X. C. Ren, P. Wang, S. H. Yu, *Sci. Rep.* **2012**, *2*, 613.
[4] J. Carretero–González, E. Castillo–Martínez, M. Dias–Lima, M. Acik, D. M. Rogers, J. Sovich, C. S. Haines, X. Lepró, M. Kozlov, A. Zhakidov, Y. Chabal, R. H. Baughman, *Adv. Mater.* **2012**, *42*, 5695.
[5] J. A. Rogers, T. Someya, Y. Huang, *Science* **2010**, *26*, 1603.
[6] Y. R. Li, K. X. Sheng, W. J. Yuan, G. Q. Shi, *Chem. Commun.* **2013**, *49*, 291.
[7] C. G. Hu, Y. Zhao, H. H. Cheng, Y. H. Wang, Z. L. Dong, C. C. Jiang, X. Q. Zhai, L. Jiang, L. T. Qu, *Nano Lett.* **2012**, *12*, 5879.
[8] R. F. Service, *Science* **2003**, *301*, 909.
[9] J. A. Rogers, Z. Bao, K. Baldwin, A. Dodabalapur, B. Crone, V. R. Raju, V. Kuck, H. Katz, K. Amundson, J. Ewing, P. Drzaic, *Proc. Natl. Acad. Sci. USA* **2001**, *98*, 4835.
[10] S. H. Ko, H. Pan, C. P. Grigoropoulos, C. K. Luscombe, J. M. J. Fréchet, D. Poulikakos, *Nanotechnology* **2007**, *18*, 345202.
[11] Y. Ahn, E. B. Duoss, M. J. Motala, X. Guo, S. I. Park, Y. Xiong, J. Yoon, R. G. Nuzzo, J. A. Rogers, J. A. Lewis, *Science* **2009**, *323*, 1590.

COMMUNICATION

[12] Y. Son, J. Yeo, H. Moon, T. W. Lim, K. H. Nam, C. P. Grigoropoulos, S. Yoo, D.-Y. Yang, S. H. Ko, *Adv. Mater.* **2011**, *23*, 3176.
[13] H. Pan, S. H. Ko, N. Misra, C. P. Grigoropoulos, *Appl. Phys. Lett.* **2009**, *94*, 071117.
[14] T. Sekitani, Y. Nouguchi, K. Hata, T. Fukushima, T. Aida, T. Someya, *Science* **2008**, *321*, 1468.
[15] S. H. Ko, H. Pan, D. Lee, C. P. Grigoropoulos, H. K. Park, *Jpn. J. Appl. Phys.* **2010**, *49*, 05EA12.
[16] K. Takei, T. Takahashi, J. C. Ho, H. Ko, A. G. Gillies, P. W. Leu, R. S. Fearing, A. Javey, *Nat. Mater.* **2010**, *9*, 821.
[17] J. Liu, M. A. G. Namboothiry, D. L. Carroll, *Appl. Phys. Lett.* **2007**, *90*, 133515.
[18] J. Ramier, C. J. G. Plummer, Y. Leterrier, J. A. E. Manson, B. Echkert, R. Gaudiana, *Renew. Energy* **2008**, *33*, 314.
[19] B. O. Connor, K. P. Pipe, M. Shtein, *Appl. Phys. Lett.* **2008**, *92*, 193306.
[20] X. Fan, Z. Chu, F. Wang, C. Zhang, L. Chen, Y. Tang, D. Zou, *Adv. Mater.* **2008**, *20*, 592.
[21] B. Weintraub, Y. Wei, Z. L. Wang, *Angew. Chem. Int. Ed.* **2009**, *121*, 9143.
[22] M. R. Lee, R. D. Eckert, K. Forberick, G. Dennler, C. J. Brabec, R. A. Gaudiana, *Science* **2009**, *324*, 232.
[23] T. Chen, L. B. Qiu, Z. B. Cai, F. Gong, Z. B. Yang, Z. S. Wang, H. S. Peng, *Nano Lett.* **2012**, *12*, 5.
[24] P. Simon, Y. Gogotsi, *Nat. Mater.* **2008**, *7*, 845.
[25] J. R. Miller, P. Simon, *Science* **2008**, *321*, 651.
[26] D. Pech, M. Brunet, H. Durou, P. Huang, V. Mochalin, Y. Gogotsi, P. Taberna, P. Simon, *Nat. Nanotechnol.* **2010**, *5*, 651.
[27] J. Bae, M. K. Song, Y. J. Park, J. M. Kim, M. L. Liu, Z. L. Wang, *Angew. Chem. Int. Ed.* **2011**, *50*, 1683.
[28] C. J. Yu, C. Masarapu, J. P. Rong, B. Q. Wei, H. Q. Jiang, *Adv. Mater.* **2009**, *21*, 4793.
[29] L. B. Hu, M. Pasta, F. L. Mantia, L. F. Cui, S. Jeong, H. D. Deshazer, J. W. Choi, S. M. Han, Y. Cui, *Nano Lett.* **2010**, *10*, 708.
[30] Y. P. Fu, X. Cai, H. W. Wu, Z. B. Lv, S. C. Hou, M. Peng, X. Yu, D. C. Zou, *Adv. Mater.* **2012**, *42*, 5713.
[31] Y. X. Xu, K. X. Sheng, C. Li, G. Q. Shi, *ACS Nano* **2010**, *4*, 4324.
[32] Z. S. Wu, A. Winter, L. Chen, Y. Sun, A. Turchanin, X. L. Feng, K. Müllen, *Adv. Mater.* **2012**, *24*, 5130.
[33] Y. Q. Sun, Q. Wu, G. Q. Shi, *Energy Environ. Sci.* **2011**, *4*, 1113.
[34] L. L. Zhang, R. Zhou, X. S. Zhao, *J. Mater. Chem.* **2010**, *20*, 5983.
[35] Y. Zhao, C. G. Hu, Y. Hu, H. H. Cheng, G. Q. Shi, L. T. Qu, *Angew. Chem. Int. Ed.* **2012**, *51*, 45.
[36] K. X. Sheng, Y. Q. Sun, C. Li, W. J. Yuan, G. Q. Shi, *Sci. Rep.* **2012**, *2*, 247.
[37] M. Hilder, B. Winther-Jensen, D. Li, M. Forsyth, D. R. MacFarlane, *Phys. Chem. Chem. Phys.* **2011**, *13*, 9187.
[38] B. Vigolo, A. Pénicaud, C. Coulon, C. Sauder, R. Pailler, C. Journet, P. Bernier, P. Poulin, *Science* **2000**, *290*, 1331.
[39] V. A. Davis, A. N. G. Parra-Vasquez, M. J. Green, P. K. Rai, N. Behabtu, V. Prieto, R. D. Booker, J. Schmidt, E. Kesselman, W. Zhou, H. Fan, W. W. Adams, R. H. Hauge, J. E. Fischer, Y. Cohen, Y. Talmon, R. E. Smalley, M. Pasquali, *Nat. Nanotechnol.* **2009**, *4*, 830.
[40] J. Bae, Y. J. Park, M. Lee, S. N. Cha, Y. J. Choi, C. S. Lee, J. M. Kim, Z. L. Wang, *Adv. Mater.* **2011**, *23*, 3446.
[41] H. J. In, S. Kumar, Y. Shao-Horn, G. Barbastathis, *Appl. Phys. Lett.* **2006**, *88*, 0831041.
[42] D. Pech, M. Brunet, P. Taberna, P. Simon, N. Fabre, F. Mesnilgrente, V. Condra, H. Durou, *J. Power Sources* **2010**, *195*, 1266.
[43] M. Kaempgen, C. K. Chan, J. Ma, Y. Cui, G. Gruner, *Nano Lett.* **2009**, *9*, 1872.
[44] L. H. Bao, X. D. Li, *Adv. Mater.* **2012**, *24*, 3246.
[45] G. Y. Zheng, L. B. Hu, H. Wu, X. Xie, Y. Cui, *Energy Environ. Sci.* **2011**, *4*, 3368.
[46] J. H. Kim, S. H. Kang, K. Zhu, J. Y. Kim, N. R. Neale, A. J. Frank, *Chem. Commun.* **2011**, *47*, 5214.
[47] J. R. McDonough, J. W. Choi, Y. Yang, F. La Mantia, Y. G. Zhang, Y. Cui, *Appl. Phys. Lett.* **2009**, *95*, 243109.
[48] Y. Li, Y. Zhao, H. H. Cheng, Y. Hu, G. Q. Shi, L. M. Dai, L. T. Qu, *J. Am. Chem. Soc.* **2012**, *134*, 15.
[49] Y. Li, Y. Hu, Y. Zhao, G. Q. Shi, L. Deng, Y. Hou, L. T. Qu, *Adv. Mater.* **2011**, *23*, 776.
[50] X. J. Xie, L. T. Qu, C. Zhou, Y. Li, J. Zhu, H. Bai, G. Q. Shi, L. M. Dai, *ACS Nano*. **2010**, *4*, 6050.
[51] L. Zhang, G. Q. Shi, *J. Phys. Chem. C*. **2011**, *115*, 17206.
[52] Y. F. Yan, Q. L. Cheng, G. C. Wang, C. Z. Li, *J. Power Sources* **2011**, *196*, 7835.